

Thermal Behavior, Morphology, and Mechanical Properties of Blend Strands Consisting of Poly(ethylene terephthalate) and Semiaromatic Liquid Crystalline Polymer

KAZUMASA YOSHIKAI,^{1,*} KAZUO NAKAYAMA,² and MUTSUMASA KYOTANI²

¹Fukuoka Industrial Technology Center, 332-1 Kamikoga, Chikushino, Fukuoka 818, Japan; ²National Institute of Materials and Chemical Research, 1-1 Higashi, Ibaraki 305, Tukuba, Japan

SYNOPSIS

Polymer blends of poly(ethylene terephthalate) (PET) and a liquid crystalline polymer (LCP) [random copolymers of the poly(ethylene terephthalate) and poly(hydroxybenzoic acid)] were prepared by using a twin-screw extruder. Strands were extruded from a capillary die. Extruded strands were stretched in an oven at 80°C. DSC and SEM were employed to investigate the structural properties of the strands. Mechanical properties of the strands were evaluated by a sonic propagation method. DSC investigation suggested that LCP phases may act as a nucleating agent of PET and the orientation-induced crystallization of PET was accelerated by the presence of LCP. An SEM micrograph shows that the LCP phases formed finely spherical domains with a diameter of 0.1–1.0 μm in the PET matrix and large parts of LCP spherical droplets were deformed to fibrils. In the case of unstretched strands, sonic moduli increased linearly with increasing LCP content, because PET was reinforced by LCP fibrils as in the case of glass fiber-reinforced PET. The degree of crystallization of PET also increased with increasing LCP contents. In the case of stretched strands, sonic moduli increased with an increasing stretching ratio due to the orientation-induced crystallization of PET. A larger increasing of the sonic modulus was shown in LCP-containing strands in the regions of a low stretching ratio (1–5), since the orientation-induced crystallization of PET was accelerated by the presence of LCP phases. © 1996 John Wiley & Sons, Inc.

INTRODUCTION

Thermotropic liquid crystalline polymers (LCP) are well-known polymers used for high-performance engineering plastics due to their excellent mechanical properties, thermal endurance, and chemical stability. Since the molecular chains of LCP easily follow the flow direction of the melt, oriented fibrous morphologies are developed in the extruded LCP. There have been many research works on the blends of LCP and other thermoplastic polymers to improve their mechanical properties.^{1–9} These studies revealed that under particular conditions LCP fabricated in the thermoplastic polymers reinforced them

as in the fiber-reinforced-plastics (FRP).^{10–15} It is also known that LCP plays the role of a nucleating agent in the blends with crystalline thermoplastic polymers.^{16,17} On the other hand, the mechanical properties of poly(ethylene terephthalate) (PET) can be improved by addition of glass fibers, and their thermomechanical properties are influenced by molecular chain orientation and crystallinity. It is expected that the mechanical properties of PET are largely enhanced by blending LCP. PET/LCP is an interesting model for polymer blends of LCP and thermoplastic polymers.

The main aim of this study was to investigate the structural and mechanical properties of polymer blends consisting of PET and LCP and the effect of the stretching of strands. The LCP, a semiaromatic copolyester [random copolymers of the poly(ethylene terephthalate) (PET) and poly(hydroxybenzoic acid)

* To whom correspondence should be addressed.

(PHB)] was selected, since the processing temperature was close to that for PET.

EXPERIMENTAL

Materials

The LCP (Rodran LC5000), composed of 20 mol % PET and 80 mol % *p*-hydroxybenzoic acid (PHB), and PET (SA-1206) were obtained from Unitika Co. The pellets of PET and LCP were dried under vacuum at 140°C for 4 h before use. Table I lists the characteristics of these materials.

Preparation of Blend Strands

The blends were prepared by a twin-screw extruder (Toyoseiki Laboplastomill) using screws ($D = 20$ mm and L/D ratio of 25). Blending temperature was 290°C. The mixing speed was fixed at 8 rpm. Blending ratios of PET/LCP (weight ratio) blends were 100/0, 90/10, 80/20, 60/40, and 0/100. Strands of blended materials were extruded from a capillary die ($D = 2$ mm, L/D ratio of 20) and cooled down in a water bath. After dried, the strands were stretched in an air oven at 80°C.

Properties

Thermal analyses of the blend strands were performed by differential scanning calorimetry (DSC) using a DSC7 (Perkin-Elmer). All runs were under a nitrogen atmosphere with a heating rate of 20°C/min. A scanning electron microscope (SEM) DS-720 (Topcon Co.) was used to analyze the mor-

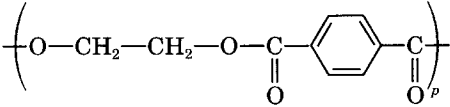
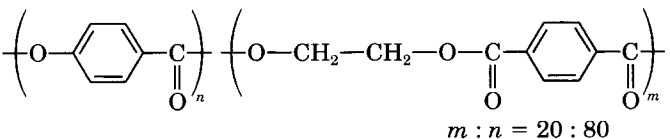
phology of the blend strands. To prepare the specimen for SEM, the strands were fractured in liquid nitrogen and fractured surfaces were coated with gold. Mechanical properties of strands were evaluated by a sonic propagation method at room temperature using a pulse propagation meter: Reovibron DDV-5-B (Orientec Co.). The pulse propagation distance between the sender and receiver of the sonic pulse at 10 kHz was 25–30 cm. The sonic modulus was calculated from the sonic velocity and the density of the strand. Densities of the blend strands were measured with a carbon tetrachloride-*n*-heptane density gradient column at 25°C.

RESULTS AND DISCUSSION

Thermal Analyses

Two kinds of transition peaks were observed in the DSC heating curves of the blend strands before stretching (Fig. 1). An exothermic peak corresponds to the cold crystallization temperature of PET and an endothermic peak corresponds to the melting temperature of PET. The glass transition temperature of PET was observed at about 70°C, but not clearly. The transition peaks of LCP were too weak to observe. The melting temperature (T_m) of the blend strands was the same as that of pure PET. The cold crystallization temperature (T_{cc}) of the blend strands was 10°C lower than that of pure PET. Figure 2 shows the dependencies of T_m and T_{cc} of the blend strands on the LCP contents. The peak shapes of the melting and the cold crystallization were not remarkably changed with the LCP contents.

Table I Characteristics of Polymers Used in This Study

Materials (Supplier)	Molecular Structure	T_m (°C)
PET (Unitika Co.)		250
RodrunLC-5000 (Unitika Co.)		270 ^a

^a Nematic transformation temperature.

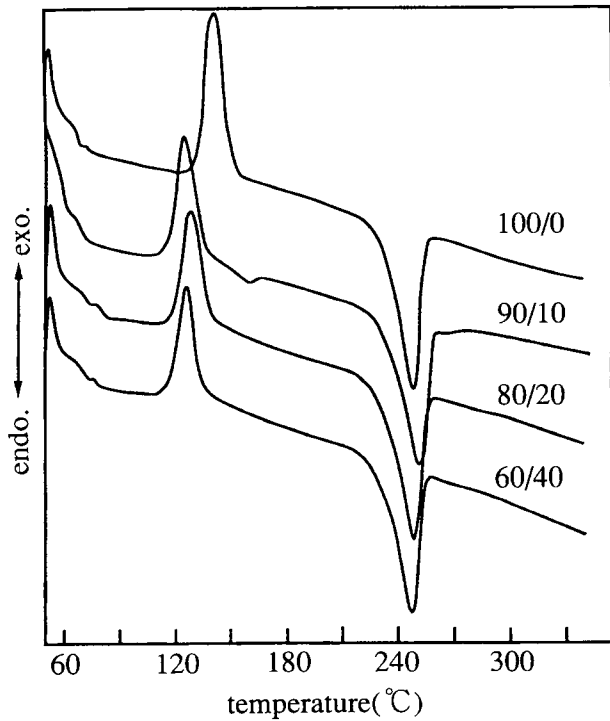


Figure 1 DSC heating curves of unstretched blend strands at a rate of 20°C/min. The blending ratios of PET/LCP are indicated.

However, the transition enthalpy was clearly changed with the LCP contents. The absolute value of the crystal melting enthalpy (ΔH_m) slightly decreased with increasing LCP content. On the other hand, the absolute value of the cold crystallization

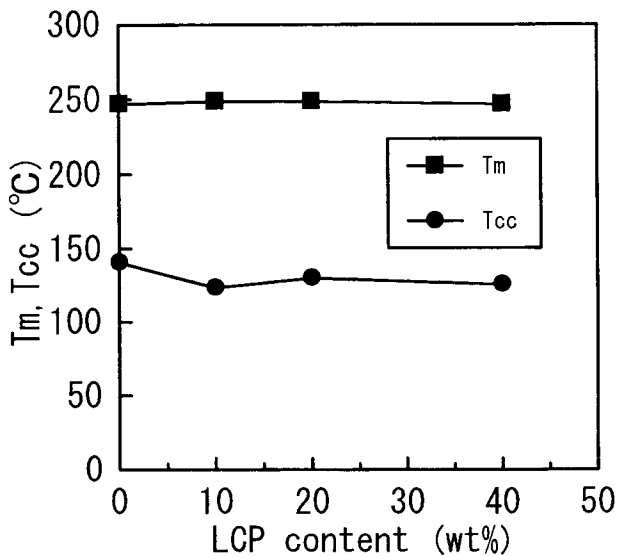


Figure 2 Changes of T_m and T_{cc} for unstretched blend strands with LCP content.

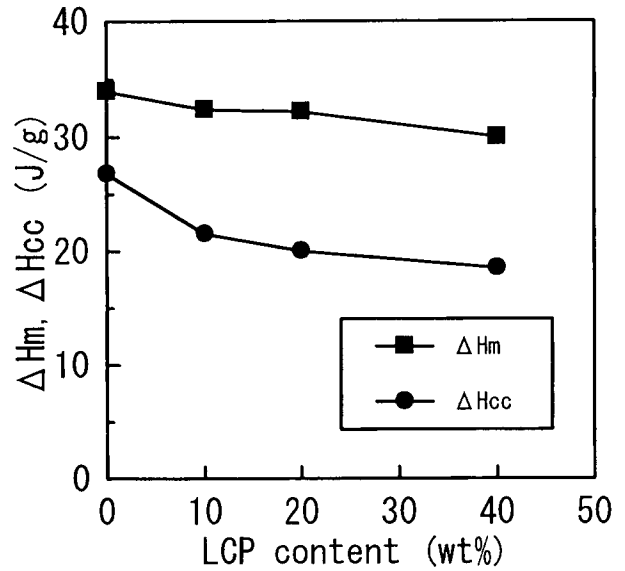


Figure 3 Changes of ΔH_m and ΔH_{cc} for unstretched blend strands with LCP content.

enthalpy (ΔH_{cc}) appreciably decreased with increasing LCP content. Therefore, $\Delta H_m - \Delta H_{cc}$, the difference between ΔH_m and ΔH_{cc} , increased with increasing LCP content. Figure 3 shows the change of ΔH_m and ΔH_{cc} as a function of LCP content. Figure 4 shows the relationship between $\Delta H_m - \Delta H_{cc}$ and LCP content. Taking into account the PET weight ratio of the blend strands, the increase of $\Delta H_m - \Delta H_{cc}$ with LCP content is more noticeable. This fact suggested that the degree of crystallinity

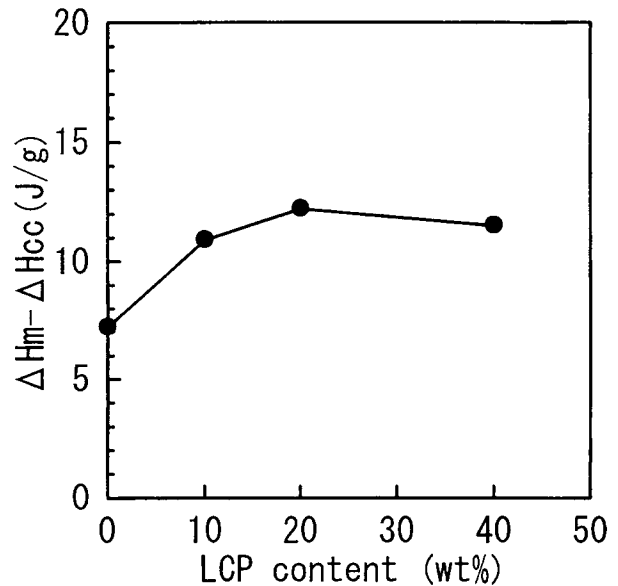


Figure 4 Relationships between $\Delta H_m - \Delta H_{cc}$ of unstretched blend strands and LCP content.

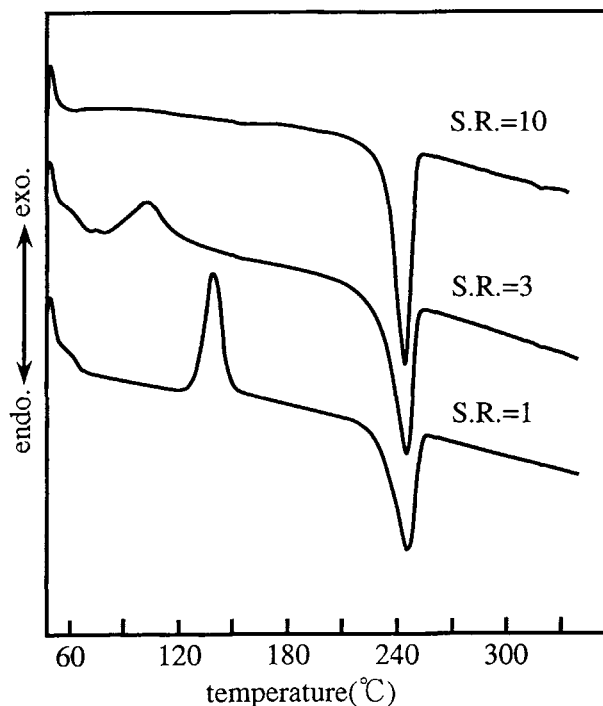


Figure 5 DSC heating curves of stretched PET strands at a rate of 20°C/min. The stretching ratios are indicated.

of PET was affected by the LCP phases, because the value of $\Delta H_m - \Delta H_{cc}$ was related to the degree of crystallinity of the strands before measurement. It should be concluded, from what has been said for the unstretched blend strands, that LCP may act as a nucleating agent for the crystallization of PET.

Figure 5 shows the DSC heating curves of stretched PET. Figure 6 shows the curves of the PET/LCP (90/10) stretched strands. T_m , evaluated as the temperature of the DSC endothermic peak, was little affected by the stretching ratio. However, the T_{cc} fell about 30°C after stretching. Figure 7 shows the changes of T_m and T_{cc} of the stretched strands as a function of the stretching ratio. The peak shapes of the transition were remarkably affected by the stretching. The sharpness of the crystal melting peak increases with an increasing stretching ratio. On the other hand, the broadening of the cold crystallization peak was observed with increasing of the stretching ratio and the T_{cc} peak disappeared at a stretching ratio of 10.

To determine the change of crystallinity of the PET matrix with the stretching of the PET/LCP blend, the transition enthalpy was evaluated. Figure 8 shows the changes of ΔH_m and ΔH_{cc} as a function of the stretching ratio. The ΔH_m increased with increasing of the stretching ratio, and the ΔH_{cc} decreased with increasing of the stretching ratio. The

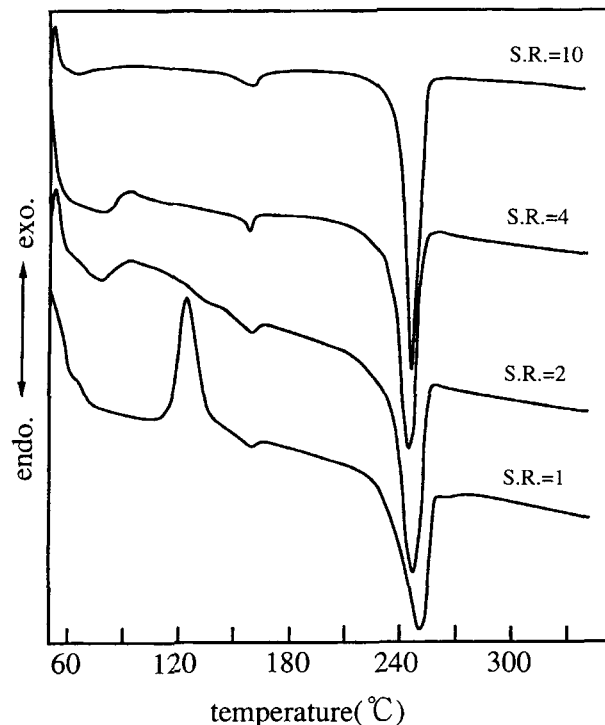


Figure 6 DSC heating curves of stretched blend strands (PET/LCP = 90/10) at a rate of 20°C/min. The stretching ratios are indicated.

value of $\Delta H_m - \Delta H_{cc}$ fairly increased with increasing of the stretching ratio (Fig. 9). It is suggested that the degree of crystallinity of PET increased with the stretching. This increase of the degree of crys-

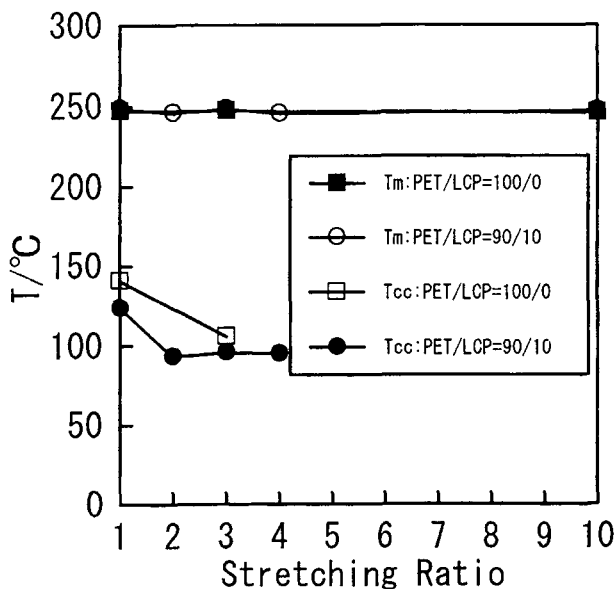


Figure 7 Relationships between T_m and T_{cc} of stretched blend strands and stretching ratio.

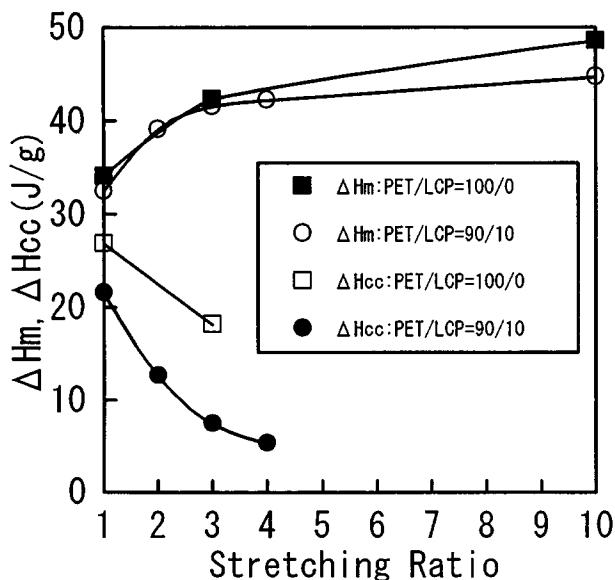


Figure 8 Relationships between ΔH_m and ΔH_{cc} of stretched blend strands and stretching ratio.

tallinity was due mainly to the orientation-induced crystallization of PET. However, in the region of the low stretching ratio, such a tendency would be more remarkable for LCP-containing strands. This tendency is more clearly shown in Figure 9. We can recognize from this fact that in the region of the low stretching ratio the orientation-induced crystallization of PET was accelerated by the presence of the LCP phases.

Morphology

The morphology of the blend strands was studied using SEM. Micrographs of skin and core portions of the fractured section of the unstretched blend strands are shown in Figure 10. Here, the skin portion means the part at 10–50 μm from the surface and the core portion means the center of strand. No clear boundary between skin and core structures was observed. Silverstein et al.¹⁸ reported the structural hierarchy in injection-molded blends of PET and LCP. Also, it is very important to know the hierarchical structure developed in the strand of PET/LCP. LCP phases formed finely dispersed spherical domains with a diameter of 0.1–1.0 μm in the PET matrix, and parts of the LCP spherical droplets were deformed to fibrils. Fibrous structures were developed near the surface of the strands. Fibrils increased with increasing LCP content. However, large parts of LCP spherical droplets were deformed in the core part of the PET/LCP (90/10) strand. It is expected that the mechanical properties of the blend

strands were improved by the LCP fibrils in such a way that glass fibers reinforced the PET. SEM micrographs of the fractured surfaces of stretched blend strands could not be obtained because successive fracturing became increasingly difficult with stretching. However, it seems that the morphology of the blend strands were little changed by the stretching, because the stretching temperature was too low to deform the LCP phases.

Mechanical Properties

The mechanical properties of the blend strands are greatly affected by the LCP contents. To determine the dependence of the mechanical properties of the PET/LCP blends on the LCP contents and stretching, the sonic moduli of strands were evaluated by $E = \rho C^2$. The sonic velocity (C) in the strand increased with increases of the LCP contents and stretching. The density (ρ) of unstretched pure PET was 1.337 g/cm^3 and that of pure LCP strands was 1.399 g/cm^3 . The density of the strands increased with LCP content. Also, the density of the blend strands increased slightly with stretching because of the increase of the crystallinity of the PET phase due to the orientation-induced crystallization. On the other hand, the sonic velocity of strands was largely affected by the increases of LCP content and the stretching ratio. Figure 11 shows the relationship between the sonic modulus ($E = \rho C^2$) of the unstretched strand and the LCP content. Before

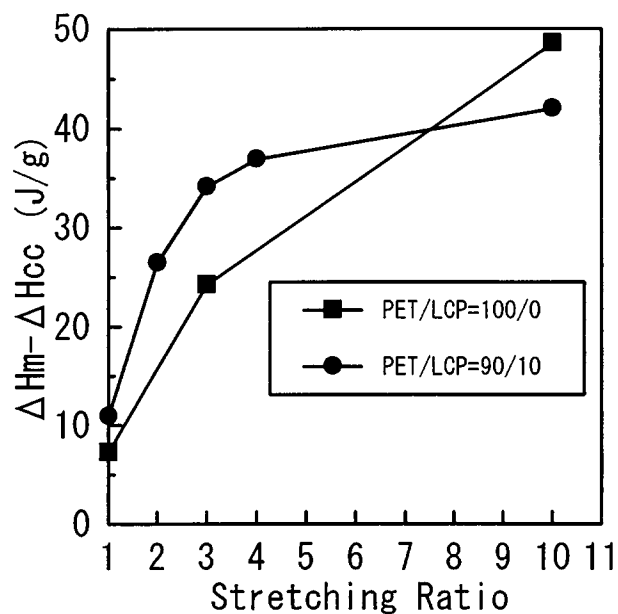
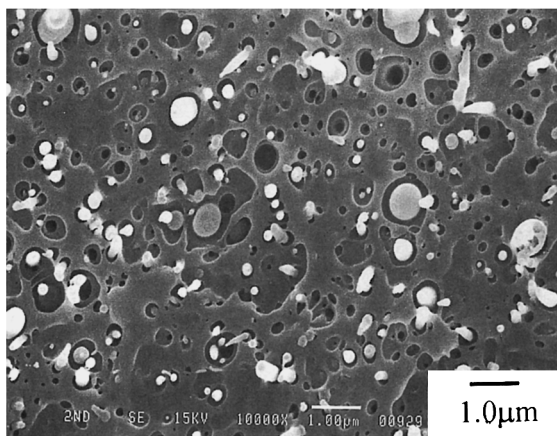
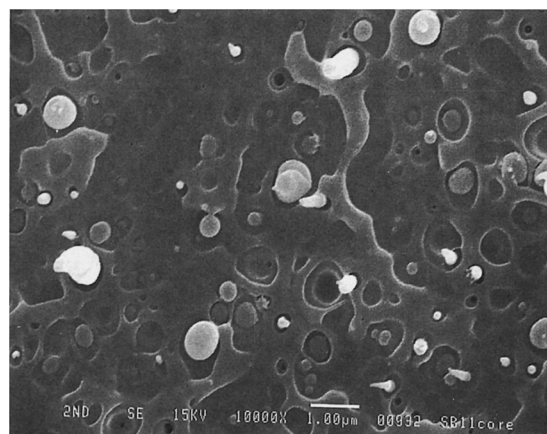


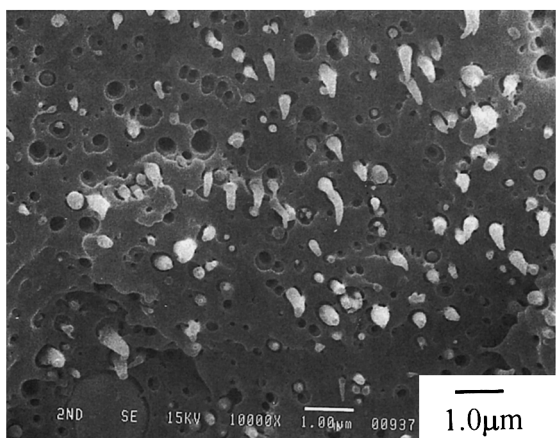
Figure 9 Relationships between $\Delta H_m - \Delta H_{cc}$ of stretched blend strands and stretching ratio.



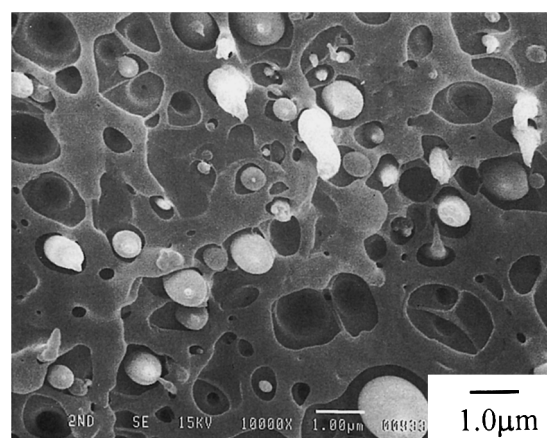
PET/LCP=90/10,skin



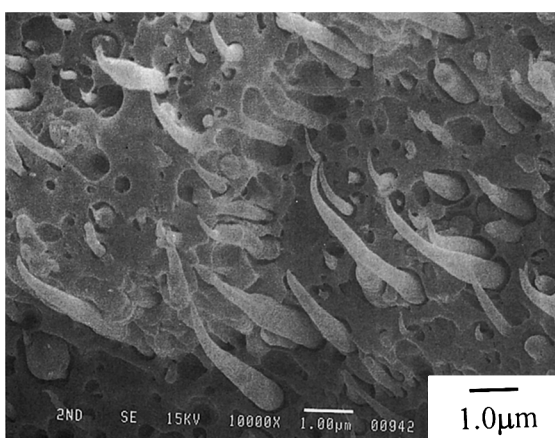
PET/LCP=90/10,core



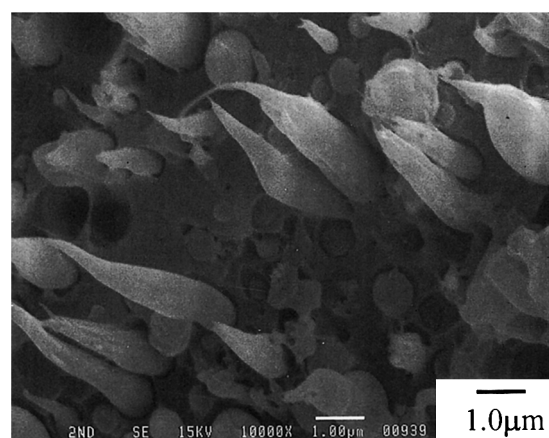
PET/LCP=80/20,skin



PET/LCP=80/20,core



PET/LCP=60/40,skin



PET/LCP=60/40,core

Figure 10 SEM micrographs of fracture surfaces of unstretched blend strands.

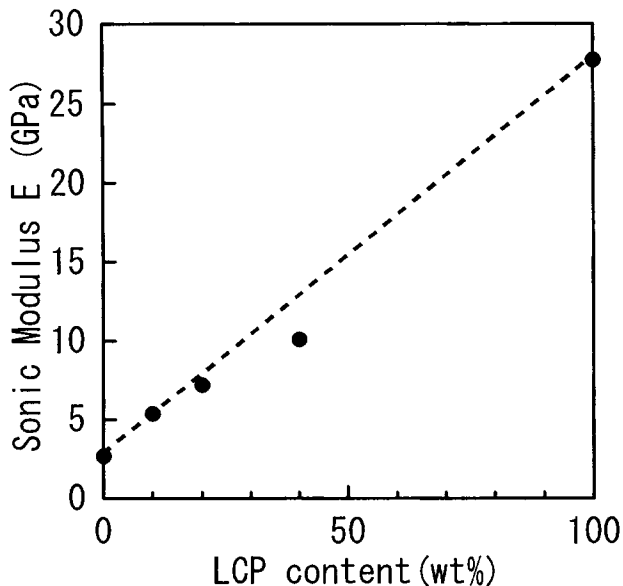


Figure 11 Relationships between sonic moduli of blend strands and LCP content.

stretching, the sonic moduli of the strands increased linearly with increasing LCP content. The data of the blend strands approximately followed the upper bound of the sonic moduli for the two-phase blends. This fact resulted from two reasons: One is that the LCP fibrils may act as glass fibers in the glass fiber-reinforced PET. The other reason is that the crystallinity of PET increases with the existence of LCP phases that may act as a nucleating agent for the crystallization of PET.

To determine the effect of stretching on the mechanical properties of the blend strands, the sonic moduli of the strands were plotted against the stretching ratio (Fig. 12). After stretching, the sonic moduli of the strands increased with the stretching ratio. In this case, the stretching of the blend strands was conducted at 80°C. This temperature is an adequate one for the stretching of pure PET. The increase of the sonic modulus of the blend strand with stretching means that the effective orientation in the PET matrix occurred. Increased orientation can lead to an improved modulus. It may also be due to the orientation-induced crystallization of PET. In the region of the low stretching ratio, greater increasing of the sonic moduli was observed in LCP-containing strands. As shown in Figure 13, this tendency is clearly shown for the stretched strands in the stretching ratio of 3. The sonic moduli of blend strands were excellent, as the data surmounted the upper bound of the moduli for the two-phase blend. It may be the result from that the degree of crystallization of PET was much higher in LCP-con-

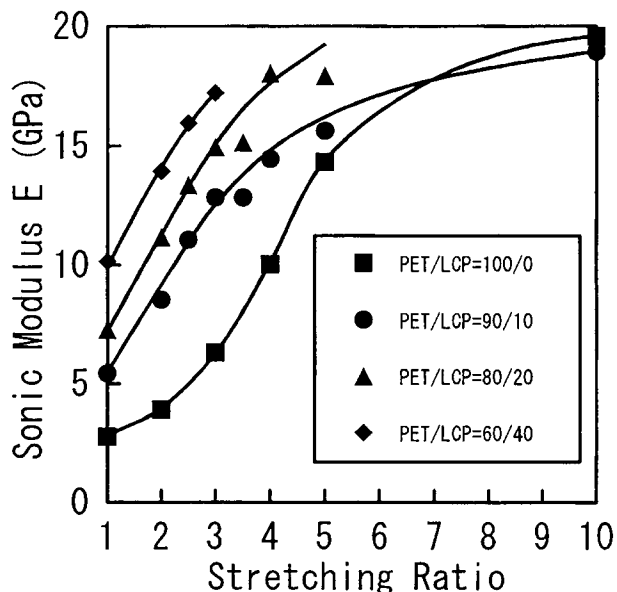


Figure 12 Relationships between sonic moduli of stretched blend strands and stretching ratio.

taining strands, as mentioned in the DSC section. At the high stretching ratio region, the tendency of the increase of the sonic moduli of LCP-containing strands was relatively small compared to pure PET. This means that the molecular chain of the PET matrix was fairly oriented at a higher stretching ratio and the improved modulus in the PET matrix became comparable with the LCP fibrils. It should be

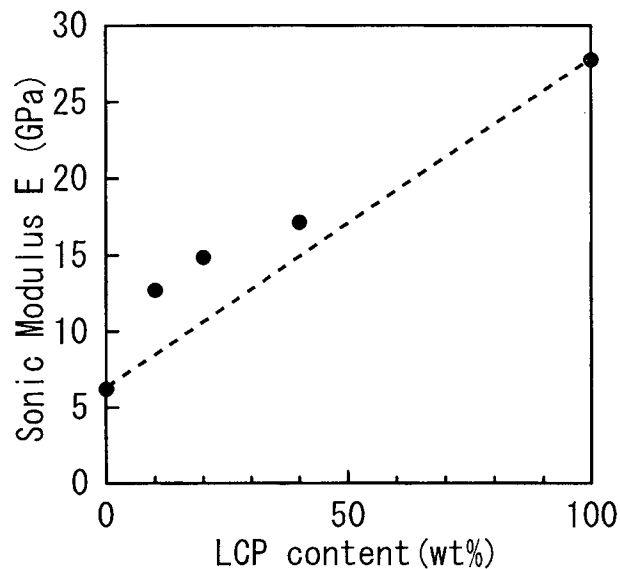


Figure 13 Relationships between sonic moduli of stretched blend strands (stretching ratio = 3) and LCP content.

concluded, from what has been said above, that the sonic moduli of PET were improved by the LCP phases through the increase of the degree of orientation and crystallinity, reinforcing by the LCP fibrils, and the increase of orientation-induced crystallinity when the strands were stretched.

CONCLUSIONS

The thermal behavior, morphology, and mechanical properties of polymer blend strands based on PET and LCP were investigated. The stretching of PET/LCP blend strands were successfully conducted at 80°C. The thermal analysis of the stretched blend strands suggests that the LCP phase may act as a nucleating agent for PET and the orientation-induced crystallization of PET was accelerated by presence of the LCP phase. The SEM micrograph shows that the LCP phases formed finely dispersed spherical domains with a diameter of 0.1–1.0 μm in the PET matrix and large parts of the LCP spherical droplets were deformed to fibrils. The sonic moduli of unstretched strands increased linearly with increasing LCP content. Two effects resulted from the LCP phases. One is that the LCP fibrils reinforce PET as do glass fibers in the glass fiber-reinforced PET. Another is that LCP phases may act as a nucleating agent for the crystallization of PET. The orientation-induced crystallization of PET causes an increase of the sonic moduli of stretched strands. In the region of the low stretching ratio, a much larger increase of the sonic moduli was observed in the LCP-containing strands, since the orientation-induced crystallization of PET was accelerated by the presence of LCP phases.

REFERENCES

1. T. Chang, *SPE 45th ANTEC Tech. Pap.*, **33**, 1404 (1987).
2. T. Chang, *Plast. Eng.*, **43**(10), 39 (1987).
3. R. Ramanathan, K. G. Blizard, and D. G. Baird, *SPE 45th ANTEC Tech. Pap.*, **33**, 1399 (1987).
4. M. Amano and K. Nakagawa, *Polymer*, **28**(2), 263 (1987).
5. S. H. Jung and S. C. Kim, *Polym. J.*, **20**(1), 73 (1988).
6. T. Harada, A. Ohara, K. Tomari, S. Tonoya, S. Nagai, and K. Yamaoka, *SPE Jpn. RETEC Tech. Pap.*, 15 (1988).
7. J. Suenaga, E. Fujita, and T. Marutani, *Kobunshi Ronbunshu*, **48**(9), 573 (1991).
8. H. Nakano, H. Yamane, Y. Kimura, and T. Kitao, *Kobunshi Ronbunshu*, **48**(6), 381 (1991).
9. M. Kimoto and T. Hiraguchi, *Kobunshi Ronbunshu*, **49**(2), 105 (1992).
10. G. Kiss, *Polym. Eng. Sci.*, **27**, 410 (1987).
11. K. Sasaki and T. Tomita, *Kobunshi Ronbunshu*, **50**(11), 855 (1993).
12. F. Yazaki, A. Kohara, and R. Yosomiya, *Kobunshi Ronbunshu*, **51**(2), 141 (1994).
13. F. Yazaki, *Kobunshi Ronbunshu*, **51**(7), 493 (1994).
14. Li-Min Sun, T. Sakamoto, S. Ueta, K. Koga, and M. Takayanagi, *Polym. J.*, **26**(8), 939 (1994).
15. Li-Min Sun, T. Sakamoto, S. Ueta, K. Koga, and M. Takayanagi, *Polym. J.*, **26**(8), 953 (1994).
16. A. M. Sukhadia, D. Done, and G. Baird, *Polym. Eng. Sci.*, **30**(9), 519 (1990).
17. M. Kyotani, A. Kaito, and K. Nakayama, *Polymer*, **33**(22), 4756 (1993).
18. M. S. Silverstein, A. Hiltner, and E. Baer, *J. Appl. Polym. Sci.*, **43**, 157 (1991).

Received January 8, 1996

Accepted April 26, 1996